Translational Oncology
www.transonc.com

Volume 12 Number 1 January 2019 pp. 8–14 8

Combined Metabolo-Volumetric Parameters of ^{18}F-FDG-PET and MRI Can Predict Tumor Cellularity, Ki67 Level and Expression of HIF 1alpha in Head and Neck Squamous Cell Carcinoma: A Pilot Study[1]

Alexey Surov[*,2], Hans Jonas Meyer[*,2], Anne Kathrin Höhn[†,2], Osama Sabri[‡,2] and Sandra Purz[‡,2]

[*]Department of Diagnostic and Interventional Radiology, University Hospital of Leipzig, Liebigstrasse 20, 04103 Leipzig, Germany; [†]Department of Pathology University Hospital of Leipzig, Liebigstrasse 20, 04103 Leipzig, Germany; [‡]Department of Nuclear Medicine, University Hospital of Leipzig, Liebigstraße 18, 04103 Leipzig, Germany

Abstract

BACKGROUND: Our purpose was to evaluate associations of combined ^{18}F-FDG-PET and MRI parameters with histopathological features in head and neck squamous cell carcinoma (HNSCC). *METHODS:* Overall, 22 patients with HNSCC were acquired (10 with G1/2 tumors and 12 with G3 tumors). ^{18}F-FDG-PET/CT and MRI was performed and maximum standardized uptake value (SUV_{max}), total lesion glycolysis (TLG) and metabolic tumor volume (MTV) were estimated. Neck MRI was obtained on a 3 T scanner. Diffusion weighted imaging was performed with estimation of apparent diffusion coefficient (ADC). Perfusion parameters K_{trans}, V_e, and K_{ep} were derived from dynamic contrast-enhanced (DCE) imaging. Different combined PET/MRI parameters were calculated as ratios: PET parameters divided by ADC or DCE MRI parameters. The following histopathological features were estimated: Ki 67, EGFR, VEGF, p53, hypoxia-inducible factor (HIF)-1α, and cell count. Spearman's correlation coefficient (p) was used for correlation analysis. $P < .05$ was taken to indicate statistical significance. *RESULTS:* In overall sample, cellularity correlated with SUV_{max}/ADC_{min} ($P = .558$, $P = .007$), TLG/ADC_{min} ($P = .546$, $P = .009$), and MTV/ADC_{min} ($P = .468$, $P = .028$). MTV/K_{ep} correlated with expression of HIF-1α ($P = .450$, $P = 0{,}047$). In G1/2 tumors, SUV_{max}/ADC_{min} correlated with HIF-1α ($P = -.648$, $P = .043$); MTV/K_{ep} ($P = -.669$, $P = .034$) and TLG/K_{ep} ($P = -.644$, $P = .044$) with Ki67. In G3 tumors, cellularity correlated with SUV_{max}/ADC_{min} ($P = .832$, $P = .001$), SUV_{max}/ADC_{mean} ($P = .741$, $P = .006$), and TLG/ADC_{min} ($P = .678$, $P = .015$). MTV/ADC_{min} and TLG/ADC_{min} tended to correlate with HIF-1α. *CONCLUSION:* Combined parameters of ^{18}F-FDG-PET and MRI can reflect Ki 67, tumor cellularity and expression of HIF-1α in HNSCC. Associations between parameters of ^{18}F-FDG-PET and MRI and histopathology depend on tumor grading.

Translational Oncology (2019) 12, 8–14

Background

Head and neck squamous cell carcinoma (HNSCC) is the most frequent malignancy of the upper aerodigestive tract in humans [1].

Different imaging modalities have been established for diagnosis and monitoring of treatment in HNSCC. Positron emission tomography (PET) with ^{18}F-fluorodeoxyglucose (^{18}F-FDG) is an imaging modality with high sensitivity in the detection of primary tumors and lymph node metastases in HNSCC [2–5]. Furthermore, ^{18}F-FDG-PET parameters like standardized uptake values (SUV), metabolic tumor volume (MTV), and total lesion glycolysis (TLG)

Address all correspondence to: Alexey Surov, Department of Diagnostic and Interventional Radiology, University Hospital of Leipzig, Liebigstrasse 20, 04103 Leipzig, Germany.
E-mail: alex.surow@medizin.uni-halle.de

[1] There was no conflict of interest.

[2] All authors contributed equally for this work.

Received 5 June 2018; Revised 25 August 2018; Accepted 29 August 2018

1936-5233/19
https://doi.org/10.1016/j.tranon.2018.08.018

can predict tumor stage and behavior of HNSCC [4–6]. It has been shown that metabolic tumor activity, measured by ^{18}F- FDG-uptake correlated with T-stage of HNSCC [4]. Also SUV can distinguish well differentiated tumors and poorly differentiated lesions: less well-differentiated tumors showed significantly higher SUVs than better-differentiated tumors [5].

Magnetic resonance imaging, especially diffusion weighted imaging (DWI) and dynamic contrast-enhanced magnetic resonance imaging (DCE-MRI) are other sensitive imaging modalities in diagnosis of HNSCC. So far, DWI by means of apparent diffusion coefficient (ADC) can predict tumor response to radiochemotherapy [7]. Also ADC values can predict lymphonodal metastasizing in HNSCC [8]. Moreover, ADC can reflect histopathological features of HNSCC, especially proliferation potential and tumor cellularity [9,10].

DCE-MRI can quantitatively characterize tumor perfusion and is associated with microvessel density in HNSCC [11]. Furthermore, DCE-MRI can predict proliferation activity in HNSCC [11].

Overall, ^{18}F-FDG-PET, DWI and DCE MRI can provide complementary information about biological features like metabolic activity, cellularity, and vascularity in HNSCC [10–14].

Numerous reports showed that combination of these modalities can better characterize primary tumors and metastatic lesions in HNSCC and estimate tumor behavior [13–16].

Furthermore, some authors suggested that several ^{18}F-FDG-PET, DWI and DCE MRI parameters can be combined together [17–19]. For example, Baba et al. calculated a new parameter, namely SUV/ADC, and showed that it had a great potential in differentiation between malignant and benign breast lesions [17]. According to Kim et al., combined parameters of ^{18}F-FDG-PET/MRI could be effective predictors of tumor treatment failure after head and neck cancer surgery [19]. Presumably, combined parameters from ^{18}F-FDG-PET and MRI may increase the diagnostic potential of the imaging and may be better associated with clinically relevant biological parameters in HNSCC than DWI, DCE-MRI and ^{18}F-FDG-PET parameters alone.

The aim of the present study was to evaluate the role of combined ^{18}F-FDG-PET/MRI parameters for prediction of different histopathological features in HNSCC.

Methods

This prospective study was approved by the institutional review board (study codes 180–2007, 201–10-12,072,010, and 341–15-05102015).

Patients

For this study, 22 patients, 6 (27%) women and 16 (73%) men, mean age, 55.2 ± 11.0 years, range 24–77 years, with different HNSCC were acquired (Tables 1a, 1b). Low grade (G1/2) tumors were diagnosed in 10 cases (45%), and high grade (G3) tumor in 12 (55%) patients.

Imaging

^{18}F-FDG-PET/CT. In all 22 patients an ^{18}F-FDG-PET/CT (Siemens Biograph 16, Siemens Medical Solutions, Erlangen, Germany) was performed from the skull to the upper thigh after a fasting period of at least 6 hours. Application of ^{18}F-FDG was performed intravenously with a body weight-adapted dose (4 MBq/kg, range: 168–427 MBq, mean ± std.: 281 ± 62.2 MBq). PET/CT image acquisition started on average 76 minutes (range 60–90 minutes) after ^{18}F-FDG application. Low-dose CT was used for attenuation correction of the PET-data.

On the same day, all 22 patients also underwent a whole body simultaneous ^{18}F-FDG PET/MRI (Biograph mMR - Biograph, Siemens Health Care Sector, Erlangen, Germany). Since simultaneous ^{18}F-FDG PET/MRI was the secondary imaging modality in the majority of the cases, start of PET/MRI image acquisition time was very inhomogeneous and varies up to 300 minutes post-injection. Since SUV values may be slightly influenced by the time-delay between the PET/CT and PET/MRI investigation due to radiotracer-clearance or further uptake, we decided to not include ^{18}F-FDG-PET-data of simultaneous PET/MRI for the current analysis to guarantee a homogenous group of patients with ^{18}F-FDG-PET image acquisition starting in a range of 60–90 minutes post-injection.

PET/CT image analysis was performed on the dedicated workstation of Hermes Medical Solutions, Sweden. For each tumor, maximum and mean SUV (SUV_{max}; SUV_{mean}), TLG and MTV were determined on PET-images. Prior to this, tumor margins of the HNSCC were identified on diagnostic CT and MRI and fused PET/CT images and a polygonal volume of interest (VOI), that include the entire lesion in the axial, sagittal and coronal planes, was placed in the PET dataset (SUV_{max} threshold 40%) (Figure 1A-D).

Diffusion-Weighted Imaging. In all patients, neck MRI was performed on a 3 T MR scanner using a combined head and neck coil. Besides anatomical sequences, an axial DWI EPI (echo planar imaging) sequence with b-values of 0 and 800 s/mm^2 (TR/TE: 8620/73 ms, slice thickness: 4 mm, and voxel size: 3.2 x 2.6 x 4.0 mm) was performed. ADC maps were automatically generated by the implemented software (Figure 1C). Regions of interest (ROI) were manually drawn on the ADC maps along the contours of the tumor on each slice (whole tumor measure, Figure 1E). In all lesions minimal ADC values (ADC_{min}) and mean ADC values (ADC_{mean}) were estimated [10].

Dynamic Contrast-Enhanced Imaging. Dynamic contrast-enhanced (DCE) imaging was performed using T1w DCE sequence (TR/TE 2.47/0.97 ms, slice thickness 5 mm, flip angle 8°, voxel size 1.2 × 1.0 × 5.0 mm) according to our previous description [11,12]. T1w DCE included 40 subsequent scans à 6 seconds. After the fifth scan, contrast medium (0.1 mmol Gadobutrol per kg of bodyweight (Gadovist, Bayer Healthcare, Leverkusen, Germany)) was administrated of started at a rate of 3 ml per second. Thereafter, the acquired images were transferred to a software module for tissue perfusion estimation (Tissue 4D, Siemens Medical Systems, Erlangen, Germany) as reported previously [11,12]. The following pharmacokinetic parameters were calculated (for exemplary parameter images see Figure 1F-H) [11,12]:

- K_{trans} or volume transfer constant representing vessel permeability. This parameter estimates the diffusion of contrast medium from the plasma through the vessel wall into the interstitial space.
- V_e or volume of the extravascular extracellular leakage space (EES);
- K_{ep} or parameter for diffusion of contrast medium from extravascular extracellular leakage space back to the plasma.

Combined parameters. In every case, the following combined PET/ADC parameters were calculated according to previous descriptions [17,19]:

- SUV_{max} divided by ADC_{min} (SUV_{max}/ADC_{min}),
- SUV_{max} divided by ADC_{men} (SUV_{max}/ADC_{mean}),

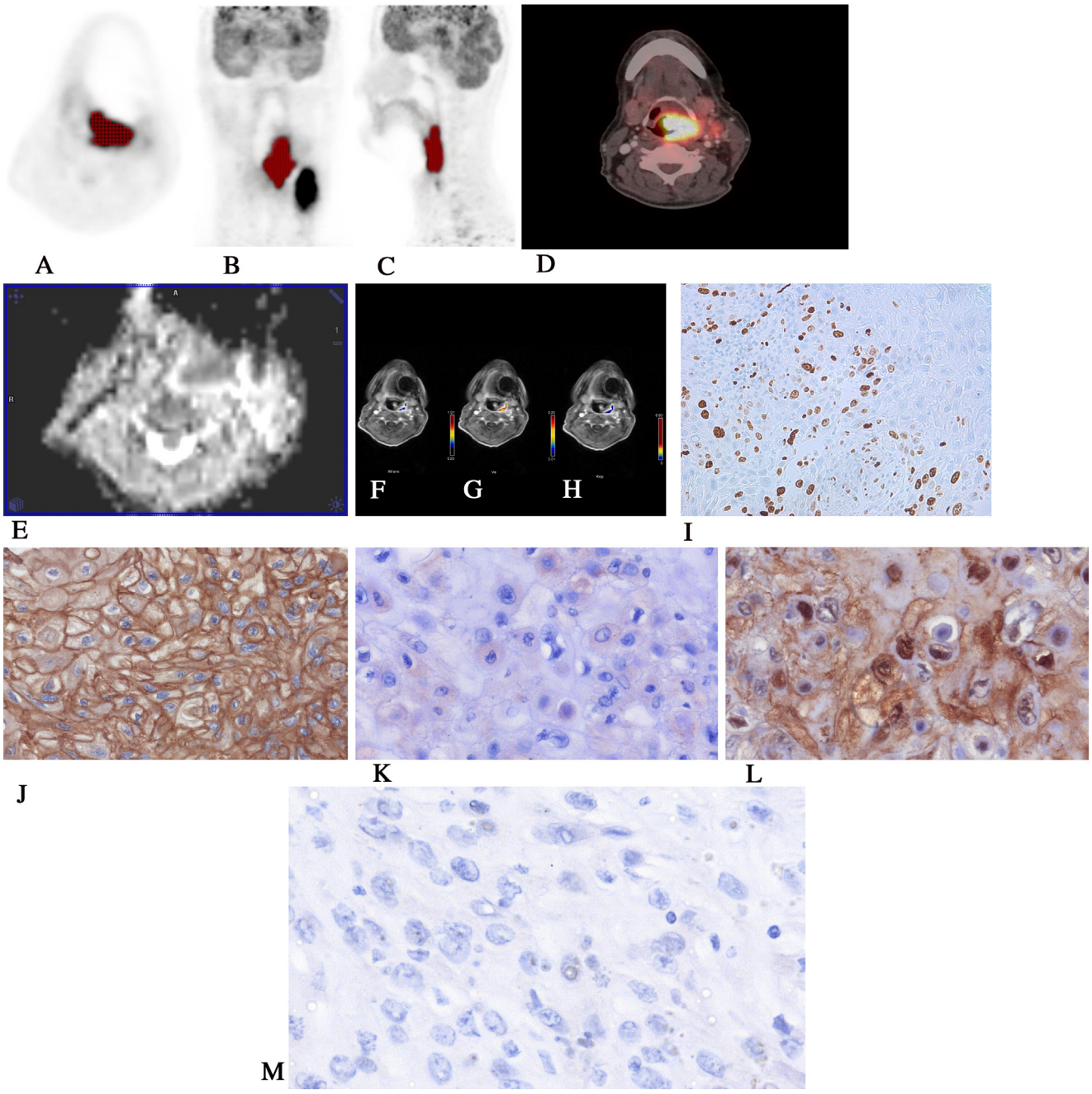

Figure 1. Imaging findings and histopathological features in a patient with metastatic HNSCC of the left oropharynx. Lesion with polygonal volume of interest (VOI, red area) in the axial (A), coronal (B) and sagittal (C) ^{18}F-FDG-PET planes. SUV_{max} = 22.6, metabolic tumor volume (MTV) = 18.12, and total lesion glycolysis (TLG) = 255.2.D. Fused 18F-FDG-PET/CT image of the lesion. E. ADC map of the tumor. The ADC values ($\times$ 10–3 mm^2 s^{-1}) of the lesion are as follows: ADC_{min} = 0.98 and ADC_{mean} = 1.5. F-H. DCE MRI images of the tumor: K_{trans} = 0.35 min^{-1} (f), V_e = 0.7% (g), K_{eP} = .61 min^{-1} (h).Histopathological parameters are as follows: I. MIB-1 staining. KI 67 index is 45%. Cell count is 121. J. EGFR staining. Stained area is 99,841 μm^2. K. VEGF staining. Stained area is 373 μm^2. L. HIF-1α staining. Stained area is 14,896 μm^2. M. p53 staining. Stained area is 0 μm^2.

- TLG divided by ADC_{min} (TLG/ADC_{min}),
- TLG divided by ADC_{mean} (TLG/ADC_{min}),
- MTV divided by ADC_{min} (SUV_{max}/ADC_{min}),
- MTV divided by ADC_{mean} (SUV_{max}/ADC_{mean}).

Furthermore, also different combined parameters PET/DCE MRI were calculated [18]. There were parameters between PET and K_{trans}:

- SUV_{max} divided by K_{trans} (SUV_{max}/K_{trans}),
- TLG divided by K_{trans} (TLG/K_{trans}),
- MTV divided by K_{trans} (MTV/K_{trans}).

Additionally, combined parameters based on associations between PET findings and V_e were calculated:

- SUV_{max} divided by V_e (SUV_{max}/V_e),
- TLG divided by V_e (TLG/V_e),

Table 1a. Associations between combined parameters PET/ADC and histopathology in HNSCC

Parameters	EGFR	VEGF	HIF-1α	p53	Ki 67	Cell count
SUV_{max}/ADC_{mean}	*P* = .081	*P* = .411	*P* = –.2	*P* = .155	*P* = .241	*P* = .403
	P = .729	*P* = .065	*P* = .385	*P* = .504	*P* = .281	*P* = .063
MTV/ADC_{mean}	*P* = .134	*P* = .009	*P* = .301	*P* = –.021	*P* = –.097	*P* = .324
	P = .563	*P* = .971	*P* = .184	*P* = .929	*P* = .668	*P* = .142
TLG/ADC_{mean}	p = .142	*P* = .132	*P* = .226	*P* = –.018	*P* = –.015	*P* = .371
	P = .54	*P* = .568	*P* = .325	*P* = .938	*P* = .946	*P* = .089
SUV_{max}/ADC_{min}	*P* = .201	*P* = .329	*P* = .056	*P* = .013	*P* = .339	**p = .558**
	P = .382	*P* = .145	*P* = .81	*P* = .955	*P* = .123	*P* = **.007**
MTV/ADC_{min}	*P* = .194	*P* = .022	***P* = .452**	*P* = –.121	*P* = .042	p = **.468**
	P = .401	*P* = .926	*P* = **.04**	*P* = .602	*P* = .851	*P* = **.028**
TLG/ADC_{min}	*P* = .166	*P* = .193	*P* = .362	*P* = –.095	*P* = .073	p = **.546**
	P = .471	*P* = .402	*P* = .106	*P* = .683	*P* = .747	*P* = **.009**

- MTV divided by V_e (MTV/V_e).

Finally, calculation of combined parameters based on associations between PET findings and K_{ep} was also made:

- SUV_{max} divided by K_{ep} (SUV_{max}/K_{ep}),
- TLG divided by K_{ep} (TLG/K_{ep}),
- MTV divided by K_{ep} (MTV/K_{ep}).

Histopathological Findings. In all cases, the diagnosis was confirmed histopathologically by tumor biopsy. The biopsy specimens were deparaffinized, rehydrated and cut into 5 µm slices.

The following histopathological features of the tumors were estimated (1i-m):

- expression of Ki 67;
- expression of epidermal growth factor receptor (EGFR);
- expression of vascular endothelial growth factor (VEGF);
- expression of tumor suppressor gene protein p53;
- expression of hypoxia-inducible factor (HIF)-1α;
- cell count.

All stained specimens were digitalized by using the Pannoramic microscope scanner (Pannoramic SCAN, 3DHISTECH Ltd., Budapest, Hungary) with Carl Zeiss objectives up to 41x bright field magnification by default. In the used bottom-up approach, the whole sample was acquired at high resolution. Via Pannoramic Viewer 1.15.4 (open source software, 3D HISTECH Ltd., Budapest, Hungary) the slides were evaluated and three captures with a magnification of x200 were extracted of each sample as reported previously [20].

Further analyses of the digitalized histopathological images were performed by using the ImageJ software 1.48v (National Institutes of Health Image program) with a Windows operating system [10,11].

Statistical Analysis

Statistical analysis was performed using SPSS package (IBM SPSS Statistics for Windows, version 22.0, Armonk, NY: IBM corporation). Collected data were evaluated by means of descriptive statistics.

Spearman's correlation coefficient (p) was used to analyze associations between investigated parameters. $P < .05$ was taken to indicate statistical significance.

Results

In overall sample, cell count correlated statistically significant with SUV_{max}/ADC_{min} (*P* = .558, *P* = 0,007), TLG/ADC_{min} (*P* = .546, *P* = 0,009), and MTV/ADC_{min} (*P* = .468, *P* = 0,028) (Table 1a). Furthermore, MTV/K_{ep} correlated with expression of HIF-1α (*P* = .450, *P* = .047) (Table 1b). There were no statistically significant correlations between other parameters.

In G1/2 tumors, SUV_{max}/ADC_{min} correlated well with expression of HIF-1α (*P* = **–**.648, *P* = .043) (Table 2a). Furthermore, MTV/K_{ep} (*P* = –.669, *P* = .034) and TLG/K_{ep} (*P* = –.644, *P* = .044) correlated with expression of Ki 67 (Table 2b). None of the combined parameters showed statistically significant correlations with cell count.

In G3 tumors, cell count correlated statistically significant with SUV_{max}/ADC_{min} (*P* = .832, *P* = .001), SUV_{max}/ADC_{mean} (*P* = .741, *P* = .006), and TLG/ADC_{min} (*P* = .678, *P* = .015) (Table 3a). Additionally, MTV/ADC_{min} and TLG/ADC_{min} tended to correlate with expression of HIF-1α (for each parameter, *P* = .6, *P* = .051). None of the PET/DCE parameters had significant correlations with the investigated histopathological features (Table 3b). Only MTV/K_{ep} tended to correlate with expression of HIF-1α (*P* = .612, *P* = .06).

Discussion

Our study showed that combined PET/MRI parameters can reflect different histopathological findings in HNSCC and, therefore, can be used as surrogate markers for tumor characterization.

Table 1b. Associations between combined parameters PET/DCE and histopathology in HNSCC

Parameters	EGFR	VEGF	HIF-1α	p53	Ki 67	Cell count
$SUVmax/K_{trans}$	*P* = –.039	*P* = .12	*P* = –.296	*P* = .158	*P* = .025	*P* = .032
	P = .87	*P* = .615	*P* = .205	*P* = .506	*P* = .915	*P* = .889
SUV_{max}/V_e	*P* = .027	*P* = .235	*P* = –.25	*P* = .214	*P* = .177	*P* = .171
	P = .91	*P* = .319	*P* = .289	*P* = .366	*P* = .443	*P* = .457
SUV_{max}/K_{ep}	*P* = –.144	*P* = .045	*P* = –.026	*P* = –.214	*P* = –.111	*P* = .056
	P = .544	*P* = .851	*P* = .915	*P* = .366	*P* = .633	*P* = .81
MTV/K_{trans}	*P* = .005	*P* = –.057	*P* = .056	*P* = .066	*P* = –.182	*P* = .156
	P = .985	*P* = .811	*P* = .816	*P* = .782	*P* = .429	*P* = .5
MTV/V_e	*P* = .104	*P* = .065	*P* = .062	*P* = .05	*P* = –.09	*P* = .278
	P = .663	*P* = .786	*P* = .796	*P* = .835	*P* = .699	*P* = .223
MTV/K_{ep}	*P* = –.078	*P* = –.088	***P* = .450**	*P* = –.308	*P* = –.23	*P* = .091
	P = .743	*P* = .711	***P* = .047**	*P* = .186	*P* = .315	*P* = .695
TLG/K_{trans}	*P* = .039	*P* = .066	*P* = –.002	*P* = .041	*P* = –.203	*P* = .209
	P = .87	*P* = .781	*P* = .995	*P* = .865	*P* = .377	*P* = .363
TLG/V_e	*P* = .126	*P* = .114	*P* = .018	*P* = .062	*P* = –.052	*P* = .33
	P = .596	*P* = .634	*P* = .94	*P* = .796	*P* = .823	*P* = .144
TLG/K_{ep}	p = –.02	*P* = –.043	*P* = .2	*P* = –.292	*P* = –.27	*P* = .064
	P = .935	*P* = .858	*P* = .398	*P* = .212	*P* = .237	*P* = .784

Significant correlations are highlighted in bold.

Table 2a. Associations between combined parameters PET/ADC and histopathology in grade 1/2 tumors

Parameters	EGFR	VEGF	HIF-1α	p53	Ki 67	Cell count
SUV_{max}/ADC_{mean}	*P* = –.176	*P* = .515	*P* = **–.794**	*P* = .248	*P* = .055	*P* = –.103
	P = .627	*P* = .128	***P* = 0,006**	*P* = .489	*P* = .88	*P* = .777
MTV/ADC_{mean}	p = .091	*P* = –.127	*P* = .115	*P* = –.418	*P* = –.62	*P* = .491
	P = .803	*P* = .726	*P* = .751	*P* = .229	*P* = .056	*P* = .15
TLG/ADC_{mean}	*P* = –.042	*P* = –.055	*P* = –.018	*P* = –.333	*P* = –.497	*P* = .527
	P = .907	*P* = .881	*P* = .96	*P* = .347	*P* = .144	*P* = .117
SUV_{max}/ADC_{min}	*P* = –.152	*P* = .467	***P* = –.648**	*P* = .067	*P* = .006	*P* = .139
	P = .676	*P* = .174	***P* = .043**	*P* = .855	*P* = .987	*P* = .701
MTV/ADC_{min}	*P* = .152	*P* = –.055	*P* = .164	*P* = –.406	*P* = –.485	*P* = .624
	P = .676	*P* = .881	*P* = .651	*P* = .244	*P* = .156	*P* = .054
TLG/ADC_{min}	*P* = .079	*P* = –.018	*P* = –.079	*P* = –.285	*P* = –.411	*P* = .527
	P = 0,829	*P* = .96	*P* = .829	*P* = .425	*P* = .238	*P* = .117

Significant correlations are highlighted in bold.

Table 2b. Associations between combined parameters PET/DCE and histopathology in grade 1/2 tumors

Parameters	EGFR	VEGF	HIF-1α	p53	Ki 67	Cell count
SUVmax/K_{trans}	p = −.176	*P* = .261	*P* = −.467	*P* = .236	*P* = −.166	*P* = −.273
	P = .627	*P* = .467	*P* = .174	*P* = .511	*P* = .647	*P* = .446
SUV_{max}/V_e	p = −.176	*P* = .176	*P* = −.43	*P* = .358	*P* = 0,215	*p* = −0,248
	P = .627	*P* = .627	*P* = .214	*P* = .31	*P* = .551	*P* = .489
SUV_{max}/K_{ep}	*P* = −.006	*P* = .152	p = −.467	*P* = −.103	*P* = −.509	*P* = −.006
	P = .987	*P* = .676	*P* = .174	*P* = .777	*P* = .133	*P* = .987
MTV/K_{trans}	*P* = −.03	*P* = −.164	*P* = .103	*P* = −.297	*P* = −.583	*P* = .406
	P = .934	*P* = .651	*P* = .777	*P* = .405	*P* = .077	*P* = .244
MTV/V_e	*P* = .115	*P* = −.115	*P* = .115	*P* = −.224	*P* = −.35	*P* = .418
	P = .751	*P* = .751	*P* = .751	*P* = .533	*P* = .322	*P* = .229
MTV/K_{ep}	p = −.03	*P* = −.079	p = .079	*p* = −.418	***P* = −.669**	*P* = .527
	P = .934	*P* = .829	*P* = .829	*P* = .229	***P* = .034**	*P* = .117
TLG/K_{trans}	p = .042	p = −.018	*p* = −.03	*P* = −.188	*P* = −.497	*P* = .321
	P = .907	*P* = .96	*P* = .934	*P* = .603	*P* = .144	*P* = .365
TLG/V_e	*P* = .055	p = .055	*P* = −.139	*P* = −.091	*P* = −.215	*P* = .345
	P = .881	*P* = .881	*P* = .701	*P* = .803	*P* = .551	*P* = .328
TLG/K_{ep}	p = .164	p = −.042	p = −.127	*P* = −.382	***P* = −.644**	*P* = .418
	P = .651	*P* = .907	*P* = .726	*P* = .276	***P* = .044**	*P* = .229

Significant correlations are highlighted in bold.

Table 3b. Associations between combined parameters PET/DCE and histopathology in grade 3 tumors

Parameters	EGFR	VEGF	HIF-1α	p53	Ki 67	Cell count
SUV_{max}/K_{trans}	p = .042	p = −.006	*P* = −.503	*P* = .188	*P* = −.073	*p* = .091
	P = .907	*P* = .986	*P* = .138	*P* = .603	*P* = .83	*P* = .79
SUV_{max}/V_e	p = .321	*P* = .175	*P* = −.309	*p* = .212	*P* = .037	*P* = .427
	P = .365	*P* = .63	*P* = .385	*P* = .556	*P* = .915	*P* = .19
SUV_{max}/K_{ep}	p = −.152	*P* = −.123	*P* = .188	*P* = −.261	*P* = .119	*P* = .118
	P = .676	*P* = .735	*P* = .603	*P* = .467	*P* = .727	*P* = .729
MTV/K_{trans}	p = .079	*P* = −.032	*P* = −.2	*P* = .503	*P* = −.119	p = −.164
	P = .829	*P* = .929	*P* = .58	*P* = .138	*P* = .727	*P* = .631
MTV/V_e	p = .164	*P* = .084	p = −.091	*P* = .418	*P* = −.083	*P* = −.036
	P = .651	*P* = .817	*P* = .803	*P* = .229	*P* = .809	*P* = .915
MTV/K_{ep}	p = −.055	*P* = −.084	*p* = .612	*p* = .042	p = .037	*P* = −.318
	P = .881	*P* = .817	*P* = .06	*P* = .907	*P* = .915	*P* = .34
TLG/K_{trans}	*P* = .224	*P* = .071	p = −.103	*P* = .394	*P* = −.046	*p* = .091
	P = .533	*P* = .845	*P* = .777	*P* = .26	*P* = .893	*P* = .79
TLG/V_e	p = .212	p = .123	p = −.055	*P* = .321	*P* = −.064	*p* = .164
	P = .556	*P* = .735	*P* = .881	*P* = .365	*P* = .851	*P* = .631
TLG/K_{ep}	*P* = .006	*P* = −.032	*P* = .43	p = −.055	*P* = −.028	*P* = −.227
	P = .987	*P* = .929	*P* = .214	*P* = .881	*P* = .936	*P* = .502

Previously, some studies investigated associations between several imaging findings and histopathology in HNSCC. However, the reported results were inconclusive. While some authors observed significant associations between imaging and histological parameters in HNSCC, others did not [10,11,21–24]. Recently, a meta-analysis regarding correlations between different imaging parameters and histopathological features in HNSCC was published [25]. It showed that SUV derived from ^{18}F-FDG PET did not correlate with Ki 67 (the pooled correlation coefficient was 0.20) [25]. Furthermore, no correlation was observed between SUV and expression of p53 (pooled correlation coefficient = 0.0). However, SUV correlated moderately with expression of HIF-1α (pooled correlation coefficient = 0.44) [25]. Regarding other imaging parameters, a statistically significant correlation between K_{trans} and Ki 67 was calculated (pooled correlation coefficient = −0.68) [25]. Also, ADC correlated well with Ki 67 (pooled correlation coefficient = −0.61) [25].

As mentioned above, some authors analyzed combined parameters from ^{18}F-FDG PET and DWI and as well from ^{18}F-FDG PET and DCE-MRI [17–19]. Overall, there were two studies about combined parameters in breast cancer [17,18] and one in HNSCC [19]. It has been shown that triple negative breast cancers showed higher metabolic–perfusion ratios, namely SUV_{max}/K_{trans}, MTV/K_{trans}, TLG/K_{trans}, and TLG/V_e, compared to non-triple negative breast cancers [18]. Furthermore, Baba et al. found that the combination of SUV and ADC, namely SUV/ADC, was more accurate than either parameter alone for differentiating benign from malignant breast lesions [17]. In HNSCC, MTV/ADC_{mean} and TLG/ADC_{mean} can predict tumor recurrence after surgical therapy, as it was shown in a study of Kim et al. [19]. Moreover, Kim et al. also showed that TLG/ADC_{mean} can predict disease-free interval and that TLG/ADC_{mean} and MTV/ADC_{mean} were associated with lymphatic invasion in HNSCC [19].

Table 3a. Associations between combined parameters PET/ADC and histopathology in grade 3 tumors

Parameters	EGFR	VEGF	HIF-1α	p53	Ki 67	Cell count
SUV_{max}/ADC_{mean}	*P* = .364	*P* = .381	*P* = −.082	p = .1	*P* = .31	***P* = .741**
	P = .272	*P* = .247	*P* = .811	*P* = .77	*P* = .327	***P* = .006**
MTV/ADC_{mean}	*P* = .318	*P* = .153	*P* = .282	*P* = .518	*P* = .077	*P* = .175
	P = .34	*P* = .654	*P* = .401	*P* = .102	*P* = .811	*P* = .587
TLG/ADC_{mean}	p = .418	*P* = .343	*P* = .245	*P* = .327	*P* = .113	*P* = .441
	P = .201	*P* = .301	*P* = .467	*P* = .326	*P* = .727	*P* = .152
SUV_{max}/ADC_{min}	p = .327	p = .21	*P* = .327	*P* = −.073	p = .5	**p = .832**
	P = .326	*P* = .536	*P* = .326	*P* = .832	*P* = .098	***P* = .001**
MTV/ADC_{min}	*P* = .255	*P* = .105	p = .6	*P* = .273	*P* = .324	*P* = .364
	P = .45	*P* = .759	*P* = .051	*P* = .417	*P* = .304	*P* = .245
TLG/ADC_{min}	p = .318	*P* = .315	*P* = 0.6	*P* = .145	*p* = .31	***P* = .678**
	P = .34	*P* = .346	*P* = .051	*P* = .67	*P* = .327	***P* = .015**

Significant correlations are highlighted in bold.

We assumed that combined parameters of ^{18}F-FDG-PET and MRI may be more sensitive than each parameter alone in reflection of histopathological features in HNSCC. In fact, our results confirmed this hypothesis. As shown, three combined PET/MRI parameters SUV_{max}/ADC_{min}, TLG/ADC_{min}, and MTV/ADC_{min} correlated statistically significant with tumor cellularity. Furthermore, MTV/K_{ep} correlated with expression of HIF-1α.

The observed associations between the combined parameters are stronger than those reported previously for PET and/or MRI parameters. For example, it has been shown that SUV_{max} did not correlate significantly with expression of Ki 67, VEGF, EGFR, HIF-1α, and p53 in HNSCC [26]. Furthermore, also the calculated PET/MRI parameters correlated better with cell count and expression of Ki 67 than ADC and/or DCE MRI parameters [27,28].

We observed also another interesting finding, namely different associations between the analyzed combined PET/MRI parameters and histopathology in dependence on tumor grading. In G1/2 tumors, SUV_{max}/ADC_{min} reflected expression of HIF-1α and MTV/K_{ep} and TLG/K_{ep} correlated strongly with expression of KI 67. In G3 tumors, SUV_{max}/ADC_{min}, SUV_{max}/ADC_{mean}, and TLG/ADC_{min} correlated strongly with tumor cellularity. It is still unknown, why associations between imaging parameters and histopathology depended on tumor grading. Presumably, tumor architecture like ratio parenchyma/stroma is different in well, moderately and poorly differentiated tumors that results in different associations between imaging and histopathology. Previously, some reports observed similar findings. For instance, it has been shown that tumor grading influenced relationships between metabolic activity, perfusion and diffusion in HNSCC [12]. Furthermore, in meningiomas, ADC correlated stronger with cellularity in grade 2/3 tumors than in grade 1 lesions [29].

Our findings have high clinical relevance. Proliferation index Ki67 is an established biomarker in HNSCC to predict tumor behavior and prognosis. High expression of Ki 67 correlated with tumoral aggressiveness and worse prognosis in patients with HNSCC [30,31]. Therefore, the possibility to estimate proliferation activity based on imaging findings is very important. Also prediction of tumor cellularity on imaging is clinically relevant and may be helpful to evaluate therapy response. Furthermore, imaging parameters may predict expression of HIF-1α, which characterizes cellular responses to hypoxic stress [32]. According to the literature, overexpression of HIF-1α is associated with increase of mortality risk and worse prognosis of HNSCC [32]. Our data suggest that the analyzed combined parameters may be used as surrogate markers in HNSCC. However, this does not apply for all histopathological biomarkers. Neither in the overall sample, nor in the subgroups the combined PET/MRI parameters correlated statistically significant with expression of p53, VEGF and EGFR. EGFR regulates many cellular processes like including proliferation, apoptosis, and differentiation [33]. It has been shown that EGFR expression can represent a good prognostic parameter in HNSCC [33,34]. Another histopathological parameter, namely tumor suppressor protein p53 regulates the activity of pathways, which lead variously to cell cycle arrest, senescence, or apoptosis following exposure of cells to endogenous or exogenous cellular stresses [35]. Finally, VEGF plays also a great role in HNSCC. It mediated different processes like endothelial cell proliferation, tumoral invasion, cell migration, chemotaxis of bone marrow derived progenitor cells, vasodilation and vascular permeability [36]. As reported previously, overexpression of this marker is a poor predictor for patients with HNSCC [30,36]. Theoretically, imaging may be associated with the mentioned biomarkers. However, as seen, combined PET/MRI parameters cannot be used for prediction of expression of p53, VEGF and EGFR. Our results are in agreement with some previous reports, in which also no associations between these histopathological biomarkers and different imaging parameters were identified [21–25].

The results of the present study are limited to a relatively small number of the acquired patients. However, this is the first report regarding associations between combined PET/MRI parameters and complex histopathological features in HNSCC. Clearly, further studies with more patients are needed to confirm our finding.

In conclusion, combined PET/MRI parameters can reflect different histopathological features, in particular KI 67, tumor cellularity and expression of HIF-1α, in HNSCC, and, therefore, can be used as surrogate biomarkers.

References

[1] Braakhuis BJ, Leemans CR, and Visser O (2014). Incidence and survival trends of head and neck squamous cell carcinoma in the Netherlands between 1989 and 2011. *Oral Oncol* **50**, 670–675.

[2] Adams S, Baum RP, Stuckensen T, Bitter K, and Hör G (1998). Prospective comparison of 18F-FDG PET with conventional imaging modalities (CT, MRI, US) in lymph node staging of head and neck cancer. *Eur J Nucl Med* **25**, 1255–1260.

[3] Ng SH, Yen TC, Liao CT, Chang JT, Chan SC, Ko SF, Wang HM, and Wong HF (2005). 18F-FDG PET and CT/MRI in oral cavity squamous cell carcinoma: a prospective study of 124 patients with histologic correlation. *J Nucl Med* **46**, 1136–1143.

[4] Haerle SK, Huber GF, Hany TF, Ahmad N, and Schmid DT (2010). Is there a correlation between 18F-FDG-PET standardized uptake value, T-classification, histological grading and the anatomic subsites in newly diagnosed squamous cell carcinoma of the head and neck? *Eur Arch Otorhinolaryngol* **267**, 1635–1640.

[5] Li SJ, Guo W, Ren GX, Huang G, Chen T, and Song SL (2008). Expression of Glut-1 in primary and recurrent head and neck squamous cell carcinomas, and compared with 2-[18F]fluoro-2-deoxy-D-glucose accumulation in positron emission tomography. *Br J Oral Maxillofac Surg* **46**, 180–186.

[6] Ryu IS, Roh JL, Kim JS, Lee JH, Cho KJ, Choi SH, Nam SY, and Kim SY (2016). Impact of (18)F-FDG PET/CT staging on management and prognostic stratification in head and neck squamous cell carcinoma: A prospective observational study. *Eur J Cancer* **63**, 88–96.

[7] Zhang Y, Liu X, Zhang Y, Li WF, Chen L, Mao YP, Shen JX, Zhang F, Peng H, and Liu Q, et al (2015). Prognostic value of the primary lesion apparent diffusion coefficient (ADC) in nasopharyngeal carcinoma: a retrospective study of 541 cases. *Sci Rep* **5**, 12242.

[8] Ai QY, King AD, Law BK, Yeung DK, Bhatia KS, Yuan J, Ahuja AT, Wong LY, Ma BB, and Mo FK, et al (2017). Diffusion-weighted imaging of nasopharyngeal carcinoma to predict distant metastases. *Eur Arch Otorhinolaryngol* **274**, 1045–1051.

[9] Driessen JP, Caldas-Magalhaes J, Janssen LM, Pameijer FA, Kooij N, Terhaard CH, Grolman W, and Philippens ME (2014). Diffusion-weighted MR imaging in laryngeal and hypopharyngeal carcinoma: association between apparent diffusion coefficient and histologic findings. *Radiology* **272**, 456–463.

[10] Surov A, Stumpp P, Meyer HJ, Gawlitza M, Höhn AK, Boehm A, Sabri O, Kahn T, and Purz S (2016). Simultaneous (18)F-FDG-PET/MRI: Associations between diffusion, glucose metabolism and histopathological parameters in patients with head and neck squamous cell carcinoma. *Oral Oncol* **58**, 14–20.

[11] Surov A, Meyer HJ, Gawlitza M, Höhn AK, Boehm A, Kahn T, and Stumpp P (2017). Correlations Between DCE MRI and Histopathological Parameters in Head and Neck Squamous Cell Carcinoma. *Transl Oncol* **10**, 17–21.

[12] Leifels L, Purz S, Stumpp P, Schob S, Meyer HJ, Kahn T, Sabri O, and Surov A (2017). Associations between 18F-FDG-PET, DWI, and DCE parameters in patients with head and neck squamous cell carcinoma depend on tumor grading. *Contrast Media Mol Imaging* , 5369625.

[13] Nakajo M, Nakajo M, Kajiya Y, Tani A, Kamiyama T, Yonekura R, Fukukura Y, Matsuzaki T, Nishimoto K, and Nomoto M, et al (2012). FDG PET/CT and diffusion-weighted imaging of head and neck squamous cell carcinoma: comparison of prognostic significance between primary tumor standardized uptake value and apparent diffusion coefficient. *Clin Nucl Med* **37**, 475–480.

[14] Fruehwald-Pallamar J, Czerny C, Mayerhoefer ME, Halpern BS, Eder-Czembirek C, Brunner M, Schuetz M, Weber M, Fruehwald L, and Herneth AM (2011). Functional imaging in head and neck squamous cell carcinoma: correlation of PET/CT and diffusion-weighted imaging at 3 Tesla. *Eur J Nucl Med Mol Imaging* **38**, 1009–1019.

[15] Choi SH, Paeng JC, Sohn CH, Pagsisihan JR, Kim YJ, Kim KG, Jang JY, Yun TJ, Kim JH, and Han MH, et al (2011). Correlation of 18F-FDG uptake with apparent diffusion coefficient ratio measured on standard and high b value diffusion MRI in head and neck cancer. *J Nucl Med* **52**, 1056–1062.

[16] Rasmussen JH, Nørgaard M, Hansen AE, Vogelius IR, Aznar MC, and Johannesen HH, et al (2017). Feasibility of Multiparametric Imaging with PET/MR in Head and Neck Squamous Cell Carcinoma. *J Nucl Med* **58**, 69–74.

[17] Baba S, Isoda T, Maruoka Y, Kitamura Y, Sasaki M, Yoshida T, and Honda H (2014). Diagnostic and prognostic value of pretreatment SUV in 18F-FDG/PET in breast cancer: comparison with apparent diffusion coefficient from diffusion-weighted MR imaging. *J Nucl Med* **55**, 736–742.

[18] An YS, Kang DK, Jung YS, Han S, and Kim TH (2015). Tumor metabolism and perfusion ratio assessed by 18F-FDG PET/CT and DCE-MRI in breast cancer patients: Correlation with tumor subtype and histologic prognostic factors. *Eur J Radiol* **84**, 1365–1370.

[19] Kim YI, Cheon GJ, Kang SY, Paeng JC, Kang KW, Lee DS, and Chung JK (2018). Prognostic value of simultaneous 18F-FDG PET/MRI using a combination of metabolo-volumetric parameters and apparent diffusion coefficient in treated head and neck cancer. *EJNMMI Res* **8**, 2.

[20] Meyer HJ, Höhn AK, and Surov A (2018). Histogram Analysis of ADC in rectal cancer: associations with different histopathological findings including expression of EGFR, Hif 1alpha, VEGF, p53, PD 1, and KI 67. A preliminary study. *Oncotarget* **9**, 18510–18517.

[21] Grönroos TJ, Lehtiö K, Söderström KO, Kronqvist P, Laine J, Eskola O, Viljanen T, Grénman R, Solin O, and Minn H (2014). Hypoxia, blood flow and metabolism in squamous-cell carcinoma of the head and neck: correlations between multiple immunohistochemical parameters and PET. *BMC Cancer* **14**, 876.

[22] Rasmussen GB, Vogelius IR, Rasmussen JH, Schumaker L, Ioffe O, Cullen K, Fischer BM, Therkildsen MH, Specht L, and Bentzen SM (2015). Immunohistochemical biomarkers and FDG uptake on PET/CT in head and neck squamous cell carcinoma. *Acta Oncol* **54**, 1408–1415.

[23] Zhao K, Yang SY, Zhou SH, Dong MJ, Bao YY, and Yao HT (2014). Fluorodeoxyglucose uptake in laryngeal carcinoma is associated with the expression of glucose transporter 1 and hypoxia inducible factor 1α and the phosphoinositide 3 kinase/protein kinase B pathway. *Oncol Lett* **7**, 984–990.

[24] Deron P, Vangestel C, Goethals I, De Potter A, Peeters M, and Vermeersch H, et al (2011). FDG uptake in primary squamous cellcarcinoma of the head and neck. The relationship between over expression of glucose transporters and hexokinases, tumour proliferation and apoptosis. *Nuklearmedizin* **50**, 15–21.

[25] Surov A, Meyer HJ, and Wienke A (2018). Can Imaging Parameters Provide Information Regarding Histopathology in Head and Neck Squamous Cell Carcinoma? A Meta-Analysis. *Transl Oncol* **11**(2), 498–503.

[26] Surov A, Meyer HJ, Höhn AK, Winter K, Sabri O, and Purz S (2018). Associations between 18F-FDG-PET and complex histopathological parameters including tumor cell count and expression of KI 67, EGFR, VEGF, HIF-1α and p53 in head and neck squamous cell carcinoma. *Mol Imaging Biol* . http://dx.doi.org/10.1007/s11307-018-1223-x.

[27] Surov A, Meyer HJ, Winter K, Richter C, and Hoehn AK (2018). Histogram analysis parameters of apparent diffusion coefficient reflect tumor cellularity and proliferation activity in head and neck squamous cell carcinoma. *Oncotarget* **9** (34), 23599–23607.

[28] Surov A, Meyer HJ, Leifels L, Höhn AK, Richter C, and Winter K (2018). Associations between histogram analysis parameters of dynamic contrast-enhanced magnetic resonance imaging and histopathological findings including proliferation potential, cellularity, and nucleic areas in head and neck squamous cell carcinoma. *Oncotarget* **9**(30), 21070–21077.

[29] Surov A, Gottschling S, Mawrin C, Prell J, Spielmann RP, Wienke A, and Fiedler E (2015). Diffusion weighted imaging in meningioma: prediction of tumor grade and association with histopathological parameters. *Transl Oncol* **8**, 517–523.

[30] Almangush A, Heikkinen I, Mäkitie AA, Coletta RD, Läärä E, Leivo I, and Salo T (2017). Prognostic biomarkers for oral tongue squamous cell carcinoma: a systematic review and meta-analysis. *Br J Cancer* **117**(6), 856–866.

[31] Gioacchini FM, Alicandri-Ciufelli M, Magliulo G, Rubini C, Presutti L, and Re M (2015). The clinical relevance of Ki-67 expression in laryngeal squamous cell carcinoma. *Eur Arch Otorhinolaryngol* **272**(7), 1569–1576.

[32] Gong L, Zhang W, Zhou J, Lu J, Xiong H, Shi X, and Chen J (2013). Prognostic Value of HIFs Expression in Head and Neck Cancer: A Systematic Review. *PLoS One* **8**(9)e75094.

[33] Bossi P, Resteghini C, Paielli N, Licitra L, Pilotti S, and Perrone F (2016). Prognostic and predictive value of EGFR in head and neck squamous cell carcinoma. *Oncotarget* **7**(45), 74362–74379.

[34] Ma X, Huang J, Wu X, Li X, Zhang J, Xue L, Li P, and Liu L (2014). Epidermal growth factor receptor could play a prognostic role to predict the outcome of nasopharyngeal carcinoma: A meta-analysis. *Cancer Biomark* **14**(4), 267–277.

[35] Tandon S, Tudur-Smith C, Riley RD, Boyd MT, and Jones TM (2010). A systematic review of p53 as a prognostic factor of survival in squamous cell carcinoma of the four main anatomical subsites of the head and neck. *Cancer Epidemiol Biomark Prev* **19**(2), 574–587.

[36] Lin X, Khalid S, Qureshi MZ, Attar R, Yaylim I, Ucak I, Yaqub A, Fayyaz S, Farooqi AA, and Ismail M (2016). VEGF mediated signaling in oral cancer. *Cell Mol Biol* **62**(14), 64–68.